Mesenchymal Bone Morphogenetic Protein Signaling Is Required for Normal Pancreas Development

Jonas Ahnfelt-Rønne,[1] Philippe Ravassard,[2] Corinne Pardanaud-Glavieux,[2] Raphaél Scharfmann,[3] and Palle Serup[1]

OBJECTIVE—Pancreas organogenesis is orchestrated by interactions between the epithelium and the mesenchyme, but these interactions are not completely understood. Here we investigated a role for bone morphogenetic protein (BMP) signaling within the pancreas mesenchyme and found it to be required for the normal development of the mesenchyme as well as for the pancreatic epithelium.

RESEARCH DESIGN AND METHODS—We analyzed active BMP signaling by immunostaining for phospho-Smad1,5,8 and tested whether pancreas development was affected by BMP inhibition after expression of Noggin and dominant negative BMP receptors in chicken and mouse pancreas.

RESULTS—Endogenous BMP signaling is confined to the mesenchyme in the early pancreas and inhibition of BMP signaling results in severe pancreatic hypoplasia with reduced epithelial branching. Notably, we also observed an excessive endocrine differentiation when mesenchymal BMP signaling is blocked, presumably secondary to defective mesenchyme to epithelium signaling.

CONCLUSIONS—We conclude that BMP signaling plays a previously unsuspected role in the mesenchyme, required for normal development of the mesenchyme as well as for the epithelium. ***Diabetes*** **59:1948–1956, 2010**

In the mouse and chicken, the pancreas originates from dorsal and ventral anlage in the endoderm, first recognized as thickenings of the epithelium which progress to form bud-like structures at e9.5 in the mouse and at e3 in the chicken embryo (1). Establishment of the pancreas territory depends on sequential signals from lateral plate mesoderm, notochord, and endothelial cells from the dorsal aorta (2–4), and requires massive rearrangements of these structures by largely unknown mechanisms. Dependent on secreted mesenchymal factors, these buds will expand and start a branching morphogenesis beginning at e12.5 in the mouse and e4 in the chicken. At the same time, the gut rotates, bringing the dorsal and ventral pancreas together, and by e12.5 in the mouse and e5.5 in the chicken, these buds have fused to form one organ (1,5). The balance between cellular differentiation and progenitor expansion is controlled by Notch signaling (6–8), and secreted mesenchymal Fgf10 appears to be involved in maintenance of the progenitor cell pool (9–11).

Few mesenchymal factors involved in pancreas development have been identified despite the long acknowledged role of epitheliomesenchymal interactions (12,13). Studies on other organ systems, such as the lung, have demonstrated that members of the transforming growth factor-β superfamily are important mediators of signals between epithelia and mesenchyme in a range of organisms (14). Several factors from this family have been reported to be expressed in the developing mouse pancreas, including bone morphogenetic proteins (BMPs) BMP4, BMP5, and BMP7 and their cognate receptors (15,16). BMP4 signaling through ALK3 was recently reported to be involved in glucose-stimulated insulin secretion in the adult pancreas (16). However, little is known about the role of BMP signaling during embryonic pancreas development.

Here we report that BMP signaling to the mesenchyme is crucial for development of the pancreas. We show that BMP signaling determined by pSmad1,5,8 immunoreactivity is restricted to the mesenchyme during early pancreas development. Inhibition of BMP signaling in vivo by Noggin results in reduced epithelial branching and increased endocrine differentiation. This coincides with a severe failure of vascular remodeling and mesenchymal morphogenesis. The effect of Noggin on endocrine differentiation can be mimicked by cell autonomous BMP signaling inhibition in the mouse pancreas mesenchyme using lentiviral transduction in vitro.

RESEARCH DESIGN AND METHODS

In ovo electroporation and in situ hybridization was performed as in previous studies (6), and at least three embryos were analyzed for each condition. RNA probes were transcribed in vitro from cDNA clones provided by BBSRC (*Bmp7*: ChEST290N8; *Bapx1*: ChEST177B22; *Pitx2*: ChEST76C15), except for the *Neurog3* cDNA provided by Anne Grapin-Botton and the *Bmp4* cDNA provided by Cliff Tabin. Probes for *Nkx6.1* and *Hes1* were used as in earlier studies (6,17) The *Xenopus Noggin* cDNA was provided by Richard Harland, and a COOH-terminal cMyc epitope tag inserted by PCR. The mouse dnALK3 was a COOH-terminal truncated receptor (encoding aa 1–237) lacking the kinase domain. A similar construct has previously been used to block BMP signaling in duck and chicken embryos (18). All expression constructs were cloned into the pCIG5 vector (6).

Whole-mount immunoflourescent staining was performed as in (19). Briefly, embryos were cleared in Dent's bleach and incubated overnight with antibodies diluted in blocking buffer. Confocal images were obtained from embryos cleared in benzyl alcohol/benzyl benzoate (BABB) (19) on a Zeiss LSM510 AxioImager. For antibodies, these data can be found in online appendix supplementary Table 1, available at http://diabetes.diabetesjournals.org/cgi/content/full/db09-1010/DC1. Perfusion of embryos with lens culinaris agglutinin was performed with a protocol modified from Jilani et al. (20). Using this protocol, the embryos were dissected in PBS, and 10 μl was injected into the heart with a pulled glass pipette. The embryos were left for

From the [1]Hagedorn Research Institute, Gentofte, Denmark; [2]Biotherapy and Biotechnology Laboratory, Centre de Recherche de l'Institut du Cerveau et de la Moelle, University Pierre et Marie Curie, Paris, France; [3]Centre de Recherche Croissance et Signalisation, Université Paris Descartes, Faculté de Médecine, Hôpital Necker, Paris, France.
Corresponding author: Palle Serup, pas@hagedorn.dk.
Received 15 July 2009 and accepted 22 May 2010. Published ahead of print at http://diabetes.diabetesjournals.org on 3 June 2010. DOI: 10.2337/db09-1010.

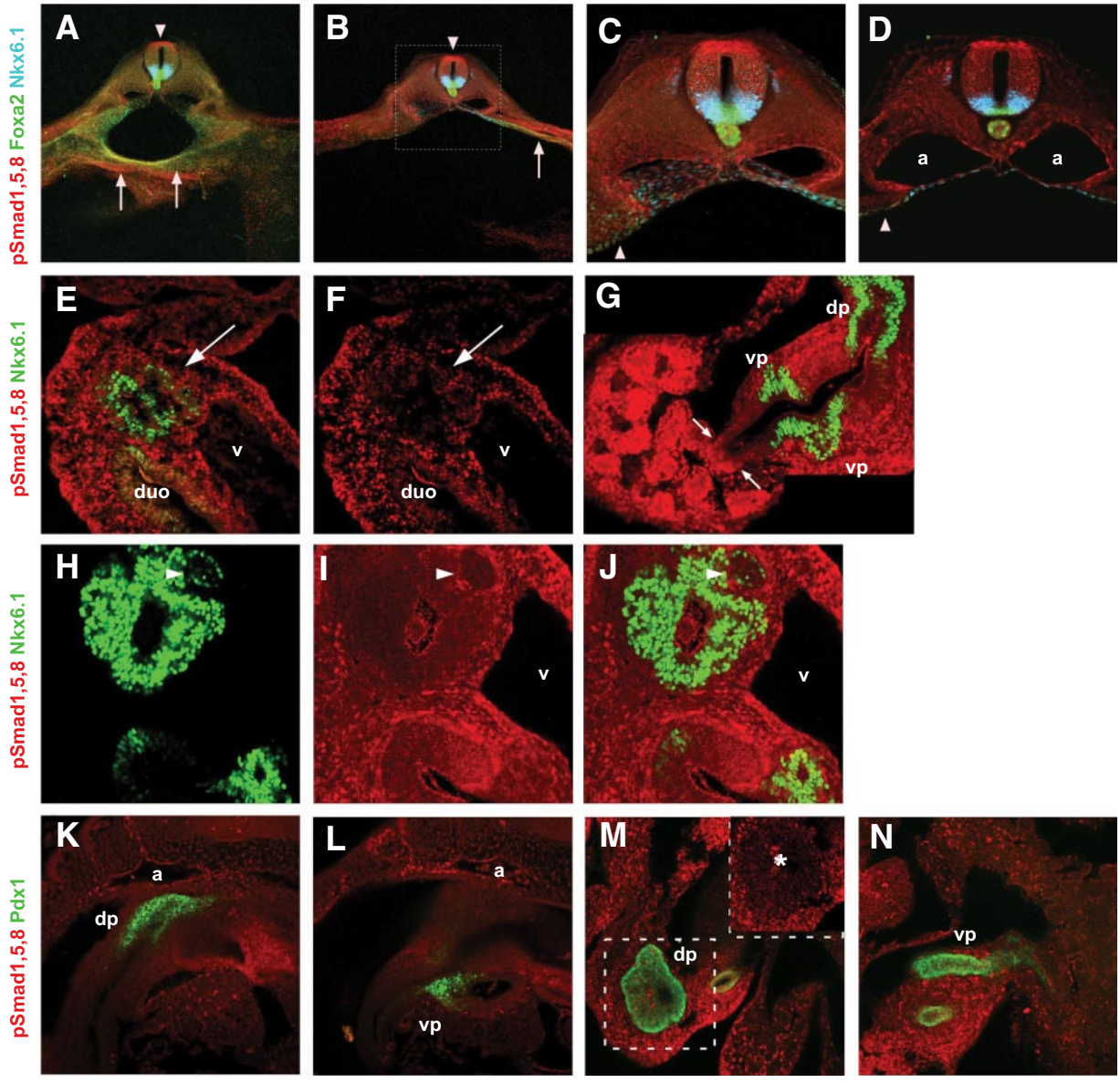

FIG. 1. pSmad1,5,8 immunoreactivity in the embryonic chicken and mouse pancreas. pSmad1,5,8 stainings on e2, e3, and e4 (HH st.12, 18, and 21) chicken embryos (*A–J*), e9.5 mouse embryo (*K–L*), and e11.5-dissected mouse gut (*M–N*). *A–D*: e2 embryo stained in whole mount as indicated. Images are either projections of confocal z-stacks of thick vibratome sections (*A–C*) or an optical section (*D*). Boxed area in *B* is shown in higher magnification in *C* and *D*. *A*: Projected image from a z-stack showing pSmad1,5,8 reactivity in the ventral forgut endoderm (*arrows*) and dorsal neural tube (*arrowhead*). *B*: Projected image at the presumptive pancreas level. Note pSmad1,5,8 reactivity in the lateral plate mesoderm and the underlying endoderm that appears yellow because of coexpression with Foxa2 (*arrow*). *C* and *D*: pSmad1,5,8 reactivity can be observed in the endothelial cells of the dorsal aortas and in endoderm lateral to the Nkx6.1 expression domain (*arrowhead*). *E* and *F*: A section of an e3 pancreas stained as indicated (shown with and without Nkx6.1). Note the pSmad1,5,8 reactivity in the mesenchyme and the absence of staining in the pancreas epithelium (*arrows* point to the dorsal pancreas). *G*: Composite of two images showing the dorsal and ventral pancreas and the liver; pSmad1,5,8 can be detected in the pancreas mesenchyme and in mesenchymal and epithelial compartments of the liver. Note the sharp boundary of pSmad1,5,8 in the bile duct (*arrows*). *H–J*: Another section from the same pancreas showing absence of pSmad1,5,8 immunoreactivity in the Nkx6.1-positive pancreatic epithelium and β-cells (recognizable by their morphology, *arrowhead*). *K* and *L*: Optical sections from a z-stack of an e9.5 mouse stained in whole mount; pSmad1,5,8 can be detected in the dorsal aorta and intersomitic vessels and in mesenchymal cells in close contact with the ventral pancreas epithelium. *M* and *N*: Optical sections from an e11.5 mouse dissected gut. Note the mesenchymal pSmad1,5,8 signal. Dashed outline is shown without Pdx1 in the inset. *marks an unspecific luminal signal from antibody trapping. a, aorta; dp, dorsal pancreas; duo, duodenum, v, right omphalomesenteric vein; vp, ventral pancreas. (A high-quality digital representation of this figure is available in the online issue.)

5 min, then fixed and processed for immunohistochemistry. Labeled areas were quantified using ImageJ software by analyzing every second optical section corresponding to an optical depth of 20 μm through the whole pancreas (between 7 and 12 sections from each embryos). Statistical significance was calculated using Student *t* test. Results were considered statistically significant if $P < 0.05$.

Lentiviral constructs were generated by gateway recombination cloning, using entry vectors with the same constructs used in the chicken experiments. Organs were cultured and transduced as by Attali et al. (21), except that the epithelium was not separated from the mesenchyme before lentiviral infection. All lentiviral vectors were used at viral concentrations corresponding to 300 ng of p24 capsid protein per explant. The e12.5-pancreas explants were fixed in formalin and embedded in paraffin 7 days after transduction. The explants were sectioned (4 μm) and stained for insulin, amylase, and DNA (DAPI) as described by Haumaitre et al. (22). Quantification was performed every fifth section spanning the entire explant using ImageJ software, and total area, insulin area, and amylase area surface were measured. In the e10.5 gut tube explants 10-μm cryosections of the entire explants were stained for insulin, amylase, and DNA (DAPI). Quantification was performed every second section by counting the nuclei of insulin and amylase-positive cells.

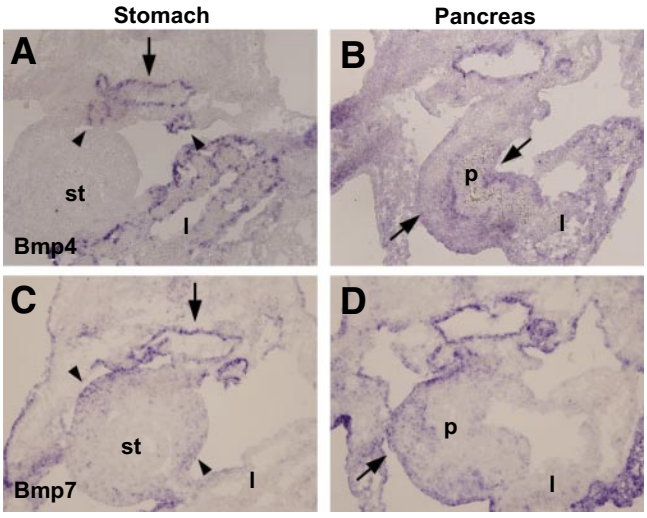

FIG. 2. Expression patterns of BMPs in the embryonic chicken pancreas—mRNA ISH, showing the expression of *Bmp4* and *Bmp7* at the level of the posterior stomach (in *A* and *C*, *arrows* point at the dorsal aorta. *Arrowheads* in *A* point to mesonephros, and *arrowheads* in *C* point to expression in the stomach mesenchyme) and the pancreas (*B* and *D*) at HH. st. 18. Note that the mesenchymal expression of *Bmp4* and *Bmp7* in the pancreas mesenchyme (*arrows*, *B* and *D*). l, liver; p, pancreas; st. stomach. (A high-quality digital representation of this figure is available in the online issue.)

We estimated total pancreatic cell numbers by adding insulin and amylase numbers. Statistical significance was calculated using Student *t* test. Results were considered statistically significant if $P < 0.05$.

RESULTS

Phospho-Smad1,5,8 immunoreactivity is restricted to the pancreas mesenchyme. BMP signaling is transduced by Smad1, −5, and −8 which, upon signaling, become phosphorylated and accumulates in the nucleus where they act as transcription factors (23). We used a phosphoSmad1,5,8-specific antibody (24) to characterize endogenous BMP signaling in the embryonic chicken pancreas (Fig. 1) at Hamburger and Hamilton (HH) stages 12, 18, and 21 (25). This corresponds to time points when the pancreas has just been specified in the endoderm, dorsal and ventral buds have formed, and α-cells, β-cells, and amylase-positive cells can be detected (6,17).

At HH st. 12, embryos were whole-mount stained and 200-μm transverse vibratome sections were analyzed (Fig. 1*A–D*). Nuclear pSmad1,5,8 could be detected in the dorsal neural tube (Fig. 1*A–D*) and in the ventral part of the anterior foregut endoderm (*arrows*, Fig. 1*A*,) as previously reported (24). At the level of the 3rd to 8th somite pairs, where the prospective pancreatic endoderm is located (3,26), pSmad1,5,8 was detected in the lateral plate mesoderm and in the endoderm lateral to the Nkx6.1 expression domain (Fig. 1*B*, *arrow*, and *arrowheads* in Fig. 1*C* and *D*, supplementary Fig. 1). We could also observe pSmad1,5,8 in the endothelium of the paired dorsal aortas (Fig. 1*C* and *D*).

At HH st. 18, pSmad1,5,8 immunoreactivity was detected in the pancreas mesenchyme and at lower levels in the duodenal epithelium (Fig. 1*E* and *F*). The dorsal pancreas epithelium was pSmad1,5,8-negative. One day later, we still observed a mesenchymal pSmad1,5,8 signal (Fig. 1*G–J*), but no signal was detected in the dorsal or ventral pancreatic epithelium. The liver epithelium had a strong signal with a sharp border of immunoreactivity in the bile duct (Fig. 1*G arrows*). No pSmad1,5,8 reactivity was detected in Nkx6.1-positive cells, which at this stage comprise both undifferentiated epithelial cells and β-cells (17) (Fig. 1*H–J*). The absence of labeling in β-cells was confirmed by colabeling with an insulin antibody (supplementary Fig. 1*G* and *H*).

To evaluate the status of Smad1,5,8 phosphorylation in the early mouse pancreas, we performed whole-mount staining at e9.5 and e11.5 for pSmad1,5,8 combined with Pdx1 (Fig. 1*K–N*). At e9.5, immunoreactivity was detected in the dorsal aortas, intersomitic vessels (Fig. 1*K* and *L*), and the dorsal neural tube (not shown). No pSmad1,5,8 was detected in the Pdx1-positive endoderm. At e11.5, we observed pSmad1,5,8 reactivity in the pancreas mesenchyme, but no reactivity in the pancreas epithelium (Fig. 1*M* and *N*). We conclude that endogenous signaling leading to detectable levels of pSmad1,5,8 in the early chicken and mouse pancreas is entirely restricted to the mesenchyme.

Several BMPs are expressed in the pancreas mesenchyme. *Bmp4*, *-5*, and *-7* mRNA have been reported to be expressed in the embryonic mouse pancreas by RT-PCR (15), and *Bmp4* and *Bmp7* have been localized to the pancreas epithelium (16), but little is known about BMP expression during chicken pancreas development. We performed in situ hybridizations at e3 (HH. st. 18) and e4 (HH. st. 22) to characterize the expression patterns of *Bmp2*, *Bmp4*, *Bmp5*, and *Bmp7* (Fig. 2 and data not shown). We found that *Bmp4* and *Bmp7* are expressed in the chicken pancreas mesenchyme and

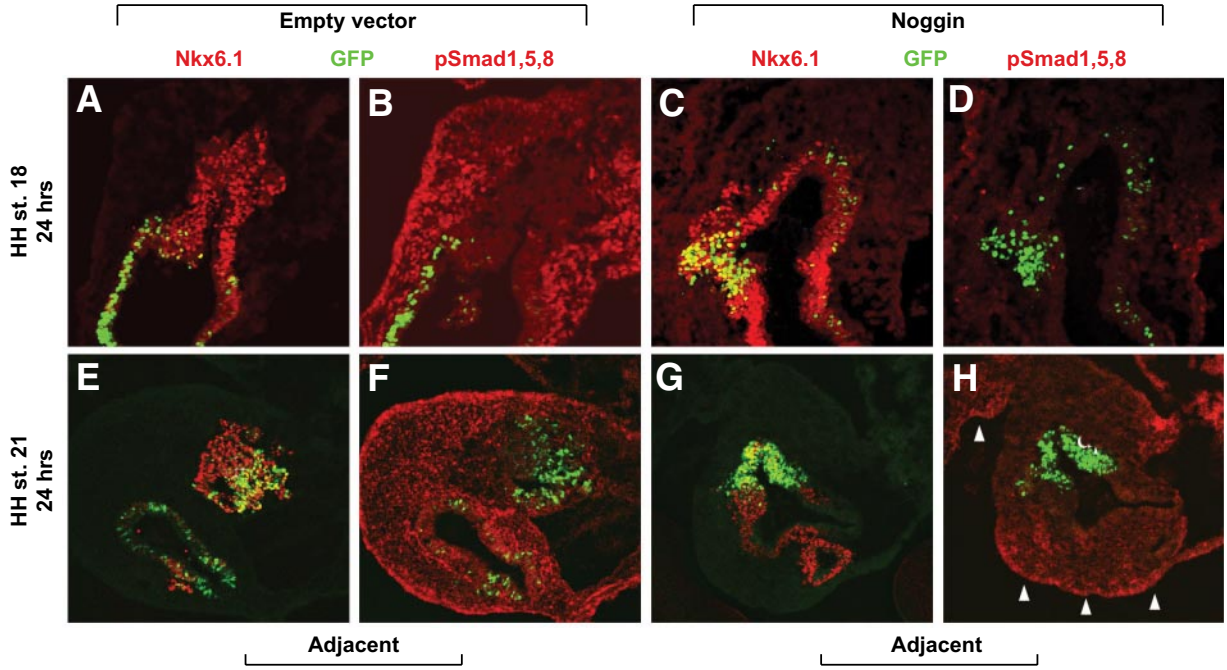

FIG. 3. Ectopic expression of Noggin in the chicken pancreas epithelium leads to loss of pSmad1,5,8 immunoreactivity in the mesenchyme. Sectioned pancreata immunolabeled as indicated, 24 h (*A–D*) and 48 h (*E–H*) after electroporation. GFP expression is showing transfected cells. Nkx6.1 is labeling the pancreas. Note the loss of pSMAD1,5,8 in the pancreas mesenchyme around the Noggin transfected area compared with controls. *H*: *Arrowheads* point to pSmad1,5,8 signals maintained at a distance from the electroporated area. dp, dorsal pancreas; vp, ventral pancreas. (A high-quality digital representation of this figure is available in the online issue.)

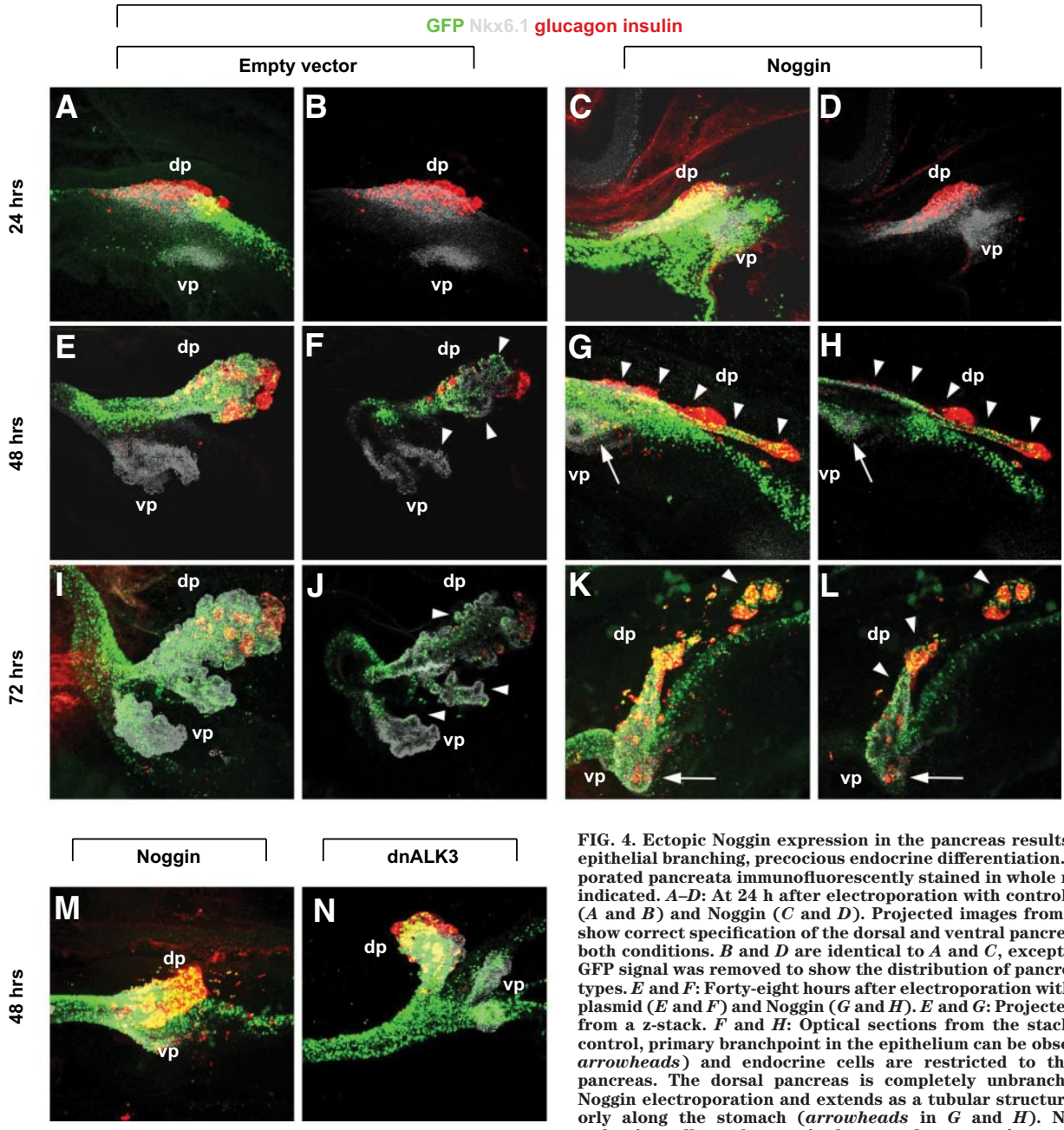

FIG. 4. Ectopic Noggin expression in the pancreas results in poor epithelial branching, precocious endocrine differentiation. Electroporated pancreata immunofluorescently stained in whole mount as indicated. *A–D*: At 24 h after electroporation with control plasmid (*A* and *B*) and Noggin (*C* and *D*). Projected images from z-stacks show correct specification of the dorsal and ventral pancreas under both conditions. *B* and *D* are identical to *A* and *C*, except that the GFP signal was removed to show the distribution of pancreatic cell types. *E* and *F*: Forty-eight hours after electroporation with control plasmid (*E* and *F*) and Noggin (*G* and *H*). *E* and *G*: Projected images from a z-stack. *F* and *H*: Optical sections from the stack. In the control, primary branchpoint in the epithelium can be observed (*F*, *arrowheads*) and endocrine cells are restricted to the dorsal pancreas. The dorsal pancreas is completely unbranched after Noggin electroporation and extends as a tubular structure anteriorly along the stomach (*arrowheads* in *G* and *H*). Numerous endocrine cells can be seen in the ventral pancreas (*arrow* in *G* and *H*). *I–L*: Seventy-two hours after electroporation with control plasmid (*I* and *J*) and Noggin (*K* and *L*). *I* and *K*: Projected images from a z-stack. *J* and *L*: Optical sections from the stack. Branching is more pronounced in the controls after 72 h (*J*, *arrowheads*), and endocrine cells are still confined to the dorsal pancreas. In Noggin electroporated pancreata, almost no branching has occurred. A large cluster of pancreatic endocrine cells can be found detached from the pancreas in the stomach mesenchyme (*K* and *L*, *arrowhead*). In the small remaining ventral pancreas, numerous endocrine cells can be observed (*K* and *L*, *arrow*). *M*: Less frequently observed phenotype 48 h after noggin electroporation—the dorsal pancreas is almost entirely converted into a large endocrine cell mass. *N*: Electroporation with dnALK3 has no effect on the normal pancreas development 48 h after electroporation. See Table 1 for quantifications. dp, dorsal pancreas; vp, ventral pancreas. (A high-quality digital representation of this figure is available in the online issue.)

excluded from the epithelium at the stages examined (Fig. 2*B* and *D* and data not shown). We could not detect *Bmp2* or *Bmp5* in the pancreas at any stage (data not shown). From these results we concluded that BMP signaling is active in the pancreas mesenchyme, possibly mediated by BMPs expressed within the mesenchyme.

Ectopic expression of Noggin in the pancreas leads to loss of pSmad1,5,8 immunoreactivity and severely affects pancreas development. To investigate the requirements for BMP signaling in pancreas development, we applied two complementary approaches. We ectopically expressed the secreted BMP antagonist Noggin or a dominant negative BMP receptor type 1 (dnALK3) in the pancreas epithelium using in ovo electroporation of the endoderm (6,27). We expected that the secreted antagonist Noggin should block BMP signaling in the epithelium as well as in the mesenchyme, whereas dnALK3 should be autonomous to the epithelial cells expressing this construct. Electroporation was performed at HH st. 10–12, and the introduced genes were thus expressed soon after the specification of the pancreas endoderm (17).

First we electroporated with a cMYC tagged Noggin in the pCIG5 vector which has an IRES nuclear enhanced green fluorescent protein (EGFP) sequence allowing direct monitoring of electroporated cells (6). As expected, EGFP was restricted to the epithelium after 32 h. However, cMYC immunoreactivity demonstrated that Noggin was efficiently secreted and spread throughout the surrounding mesenchyme (supplementary Fig. 2). We next assayed for pSmad1,5,8 in the pancreas 24 and 48 h after electroporation (Fig. 3). Electroporation with a control plasmid did not change the pattern of endogenous pSmad1,5,8 (Fig. 3*B* and *F*), but ectopic expression of Noggin resulted in loss of mesenchymal pSmad1,5,8 immunoreactivity around the electroporated area (Fig. 3*D* and *H*). We could still detect pSmad1,5,8 in the

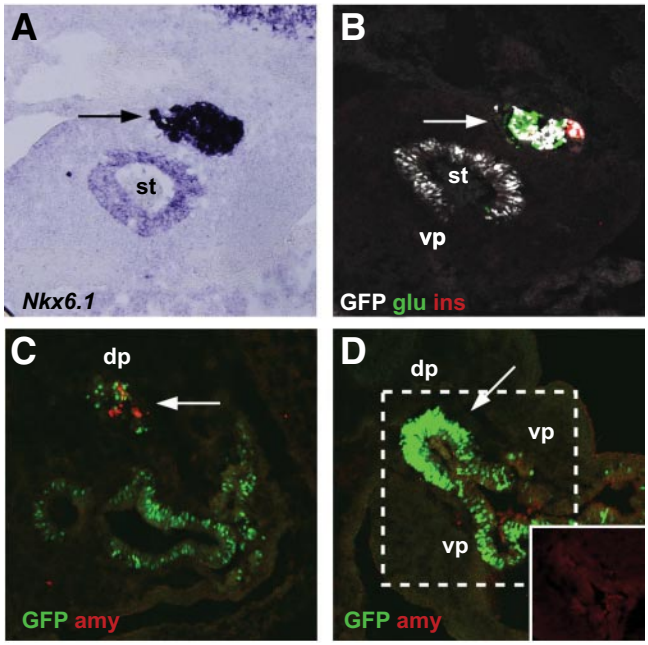

FIG. 5. Pancreatic cell types can be observed in the stomach mesenchyme and exocrine differentiation is reduced 48 h after electroporation with Noggin. *A* and *B* are adjacent sections at the level of the stomach in a Noggin electroporated embryo showing Nkx6.1 mRNA expression and insulin and glucagon protein expression, respectively. Large clusters of pancreatic cells can be found in the stomach mesenchyme, and both glucagon and insulin are readily found (*A* and *B*). *C* and *D*: Sections of the pancreas of control (*C*) and Noggin (*D*) electroprated embryos imunoflurescently labeled for Amylase and showing GFP expression in electroporated cells. in *D inset*: The boxed area is without GFP. Note the absence of amylase-positive cells in the Noggin-electroporated pancreas. (A high-quality digital representation of this figure is available in the online issue.)

mesenchyme at a distance from the electroporated area (Fig. 3*H*, *arrowheads*) and in the dorsal neural tube (not shown). We noted that the Nkx6.1-positive pancreas epithelium appeared less developed than the corresponding controls after 48 h (compare Fig. 3*G–E*).

To assess pancreas morphogenesis, we performed whole-mount immunofluorescent staining of electroporated embryos at 24, 48, and 72 h. Three-dimensional projections of confocal z-stacks were generated showing green fluorescent protein (GFP), Nkx6.1, and glucagon/insulin (Fig. 4). At 24 h after electroporation with control plasmid or Noggin, the dorsal and ventral pancreata were both formed normally, and endocrine cells were found exclusively in the dorsal pancreas (Fig. 4*A–D*). At 48 h, the pancreata electroporated with empty vector developed normally with primary branching, two distinct ventral pancreas buds (5), and endocrine cells confined to the dorsal pancreas (Fig. 4*E* and *F*). In contrast, development of the Noggin electroporated pancreata was severely disturbed (Fig. 4*G*, *H*, *M*). There was no primary branching of the epithelium. Instead the dorsal pancreas appeared as a tubular structure extending anteriorly along the stomach (Fig. 4*G* and *H*). Quantifying the amount of epithelial and endocrine areas showed that the total endocrine area was unchanged, but the epithelium was reduced by ~50% (supplementary Table 2). Precocious endocrine cells could be observed in the ventral pancreas which was hypoplastic (Fig. 4*G* and *H*, *arrow*; supplementary Table 2). In some embryos, the pancreas was almost entirely converted into a large endocrine cluster (Fig. 4*M*).

At 72 h after electroporation with control vector, endocrine cells were still confined to the dorsal pancreas and branching of the epithelium was prominent (Fig. 4*I* and *J*). Conversely, the pancreata of Noggin electroporated embryos were hypomorphic, and large endocrine clusters detached from the pancreas could be observed in the stomach mesenchyme (Fig. 4*K* and *L*, *arrowheads*). There was no epithelial branching and endocrine cells were found in the ventral pancreas (Fig. 4*K* and *L*, *arrow*). Cell-autonomous inhibition of BMP signaling in the endoderm via electroporation with dnALK3 had no effect on pancreas development (Fig. 4*N*), suggesting that the effect elicited by Noggin is through inhibition of BMP signaling in the mesenchyme. In neural tube electroporation experiments, dnALK3, as well as Noggin, was able to block Smad1,5,8 phosphorylation in the dorsal neural tube. confirming that the dnALK3 construct worked as expected (supplementary Fig. 2*C–H*).

The pancreas of Noggin electroporated embryos was further analyzed on sections 48 h after electroporation (Fig. 5). The anterior extension of the pancreas contained Nkx6.1, glucagon, and insulin-positive cells (Fig. 5*A* and *B*). Control pancreata contained scattered exocrine cells marked by amylase

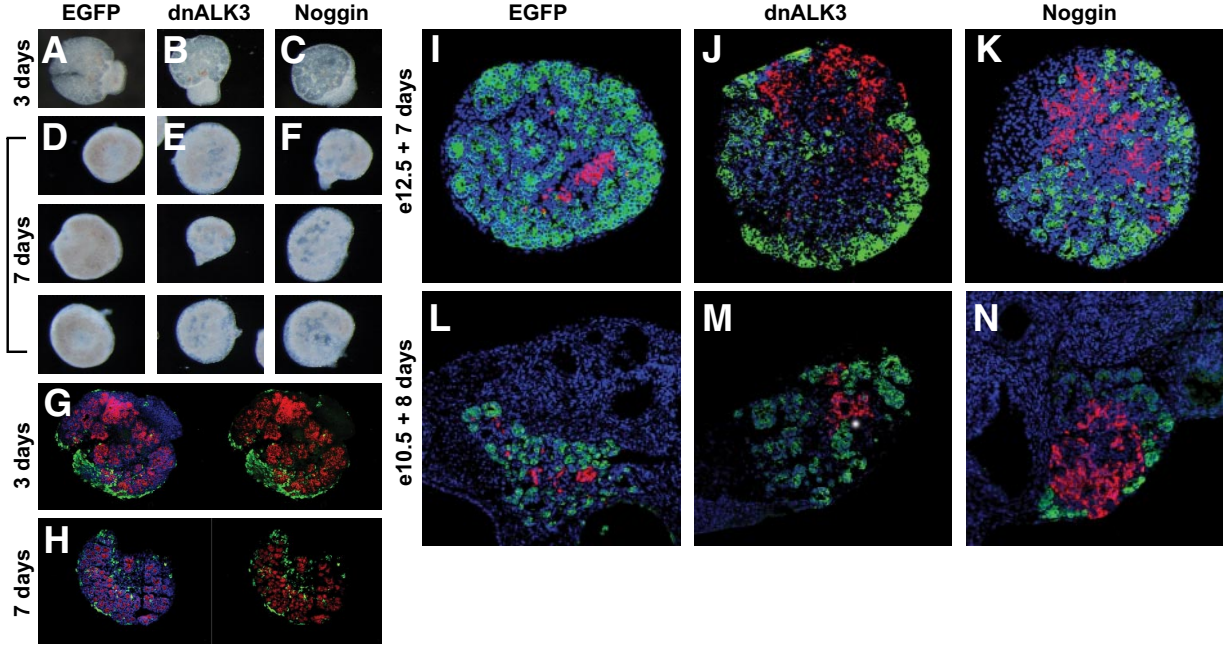

FIG. 6. Cell autonomous BMP signaling inhibition in the mouse pancreas mesenchyme results in increased β-cell differentiation. Mouse pancreas organ cultures explanted and transduced at e12.5 (*A–K*) or 10.5 (*L–N*) with lentiviral constructs as indicated. *A–C*: Stereomicrographs after 3 days in culture. *D–F*: Stereomicrographs of three different explants of each condition after 7 days in culture. *G* and *H*: Explants transduced with a control EGFP construct, immunflurescently stained for E-cadherin (red) and showing EGFP with or without DAPI nuclear counterstain. Note how GFP expression is restricted to the mesenchyme 3 and 7 days after transduction. *I–K*: Explants transduced as indicated and cultured for 7 days. Immunostained for amylase (green), insulin (red), and nuclei (DAPI, blue). *L–N*: Explants transduced at e10.5 and cultured for 8 days, then stained for amylase and insulin with DAPI nuclear counter stain. See Table 2 for quantifications. (A high-quality digital representation of this figure is available in the online issue.)

expression (Fig. 5*C*), but no exocrine cells were found in Noggin electroporated embryos (Fig. 5*D*).

Cell-autonomous BMP inhibition in the mesenchyme has a similar effect on endocrine and exocrine differentiation as BMP inhibition by Noggin. The results presented so far indicate that BMP signaling is required in the mesenchyme and that the effect on the epithelium is indirect. This was difficult to demonstrate directly since electroporation in the chicken embryo does not permit cell-autonomous inhibition of BMP signaling in the mesenchyme. Therefore, we took advantage of established protocols for in vitro development of mouse pancreas explants and lentiviral gene transduction (28). We explanted e12.5 pancreata transduced with lentivirial vectors encoding either GFP, Noggin, or dnALK3. When whole pancreas explants were exposed to lentiviral vectors, exclusive infection of the mesenchyme was achieved (Fig. 6*H* and *I*), allowing inhibition of mesenchymal BMP signaling in a cell-autonomous manner with dnALK3.

The explants were cultured for 3 or 7 days (Fig. 6*A–F*). Stereomicrographs of the explants cultured for 7 days showed that dnALK3 and Noggin-transduced explants had a similar morphology and were of similar size as controls (Fig. 6*A–F*). Costaining for E-cadherin and GFP on GFP-transduced explants confirmed the mesenchymal-specific expression after 3 and 7 days in culture (Fig. 6*H* and *I*). We quantified the number of exocrine cells and β-cells after 7 days in culture (Fig. 6*J–L*, supplementary Table 3) and found a 2.8-fold increase in the relative area of β-cells in dnALK3-transduced explants compared with controls. This expansion was even more pronounced in Noggin-transduced explants which showed a 3.6-fold increase in relative β-cell area. In contrast, the relative exocrine area was diminished in dnALK3 and Noggin-transduced explants compared with controls (not statistically significant). There was no obvious branching defect in these studies, which could be a result of different timing of BMP inhibition compared with the studies performed in chicken. We therefore repeated the experiments with e10.5 explants prior to branching morphogenesis. E10.5 gut tubes were dissected; transduced with GFP, Noggin, or dnALK3; and cultured for 4 and 8 days. After 4 days, the total explant volume was reduced by 5.5- and 1.8-fold when transduced with Noggin and dnALK3, respectively (compared with control GFP transduction; supplementary Fig. 3*E*). Noggin transduction resulted in a subtle change in the overall branching pattern, visualized by whole-mount Mucin-1 staining, as main ducts were not well defined and appeared diffuse compared with controls (supplementary Fig. 3*A–D*). After 8 days in culture, mesenchymal Noggin expression increased the total number of insulin-positive cells by 3.8-fold, whereas the total number of amylase-positive cells were reduced by 1.6-fold (Fig. 6*M–O*, supplementary Table 3). Similarly, mesenchymal expression of dnALK3 increased the number of insulin-positive cells by 2.5-fold, demonstrating that cell autonomous BMP signal reception in the mesenchyme is required for a normal rate of endocrine cell differentiation to occur. We did observe a small but statistically significant effect on total exocrine cell numbers in Noggin-transduced explants and in relative numbers of exocrine cells in both Noggin and dnALK3 transduced (supplementary Table 3). The effect of mesenchymal expression of dnALK3 on branching morphogenesis was ambiguous; some explants exhibited a phenotype similar to the Noggin-transduced explants, whereas some had a normal appearance (not shown). We speculate that this may be attributed to variable transduction efficiency.

Mesenchymal gene expression is severely affected by Noggin-mediated BMP inhibition. Since our results suggested that Noggin inhibited BMP signaling in the mesenchyme, we next investigated mesenchymal gene expression patterns. *Pitx2* is normally expressed in the left side of the mesenchyme of vertebrate embryos and is involved in asymmetrical organ development (29,30). *Bapx1* was recently demonstrated to be involved in the left-sided lateral growth of the e10.5 mouse dorsal pancreas because of a requirement for *Bapx1* in the formation of a specialized mesothelial structure, the splancnic mesodermal plate (SMP) (31). It is normally expressed in the left side of the mesenchyme, and it is required for the separation of the splenic and pancreatic mesenchyme and maintenance of the pancreas character in the distal part of the dorsal pancreas (31,32). To evaluate the expression of *Pitx2* and *Bapx1* in relation to the chicken pancreas, we first performed mRNA in situ hybridizations on serial sections for *Nkx6.1* and *Shh*, together with *Pitx2* and *Bapx1* (supplementary Fig. 4). We found that, as in the mouse, *Bapx1* was initially expressed bilaterally in the pancreas region (supplementary Fig. 4*P*), but from e3 strong expression was restricted to the *Pitx2*-positive mesenchyme on the left side of the pancreas (supplementary Fig. 4*I*, *J*, *L*, and *M*). *Bapx1* appeared to be symmetrically expressed at the level of the stomach (supplementary Fig. 4*H*) as in the mouse (31).

In control embryos, we found that *Bapx1* was expressed left sided in the pancreas mesenchyme together with *Pitx2* after 48 h (Fig. 7*C* and *E*). In contrast, Noggin-electroporated embryos displayed a duplication of *Bapx1* expression, whereas *Pitx2* remained left sided, suggesting that *Bapx1* and *Pitx2* expression is uncoupled at least under these conditions (Fig. 7*D* and *F*).

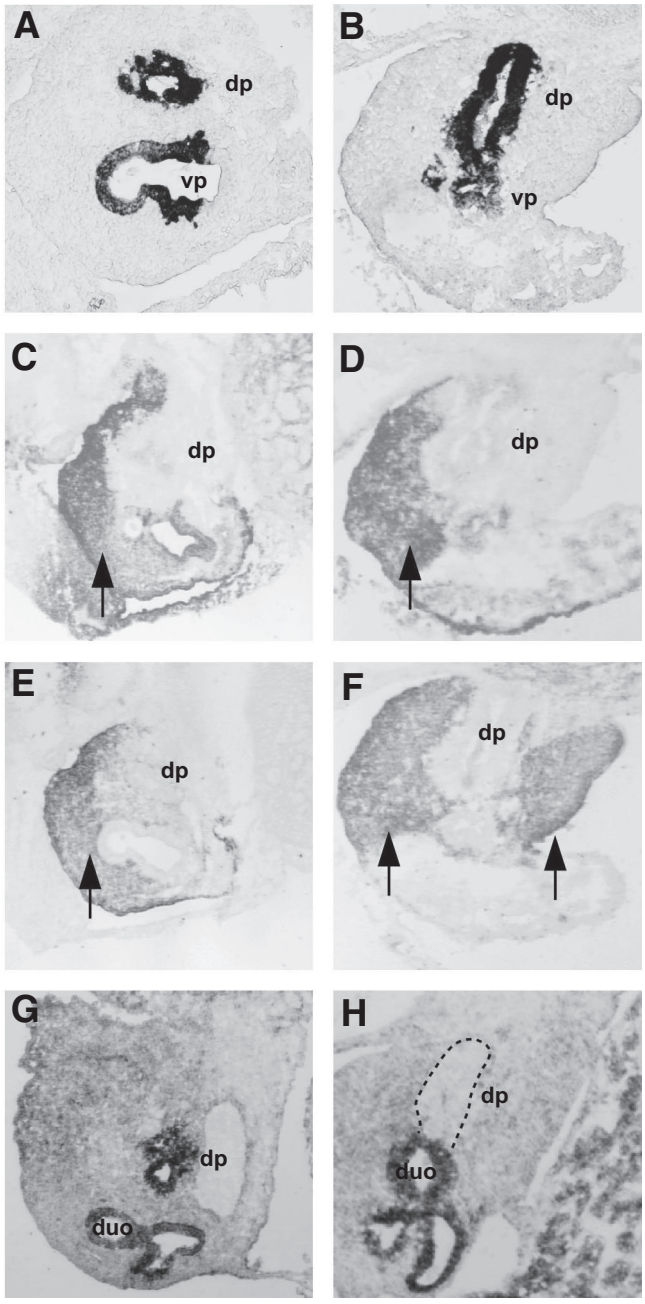

FIG. 7. Electroporation with Noggin results in persistence of a *Bapx1*-positive pancreas mesenchyme on the right side of the pancreas 48 h after electroporation. mRNA in situ hybridization on electroporated embryos 48 h after electroporation. *A*, *C*, *E* and *B*, *D*, *F* are serial sections from the same embryos, *G–J* are serial sections from other embryos. *Nkx6.1* staining shows the pancreas epithelium (*A* and *B*). *Pitx2* and *Bapx1* are normally coexpressed on the left side of the pancreas in control embryos (*arrows*, *C* and *E*). However, in Noggin-electroporated embryos, *Bapx1* expression becomes symmetrically expressed on both sides of the pancreas (*arrows*, *F*), whereas Pitx2 remains left sided (*arrow*, *D*). Most of the unbranced dorsal pancreas in Noggin electroporated embryos does not express *Hes1* (*G* and *H*), but the duodenum maintains *Hes1* expression. dp, dorsal pancreas; duo, duodenum; vp, ventral pancreas.

These results are in agreement with a role for BMP signaling in development of the pancreas mesenchyme. Since *Bapx1* is involved in the formation of the SPM in the mouse embryo, we hypothesized that this structure could be affected in the BMP-inhibited embryos. We therefore stained for Isl1 and laminin or Nkx6.1/Nkx2.2 with DAPI nuclear counter stain to visualize this structure (supplementary Fig. 5). In control embryos, the SPM was asymmetric with a condensation of the mesothelium on the left side at HH st. 19, 32 h after electroporation (supplementary Fig. 5*A* and *B*). Noggin electroporated

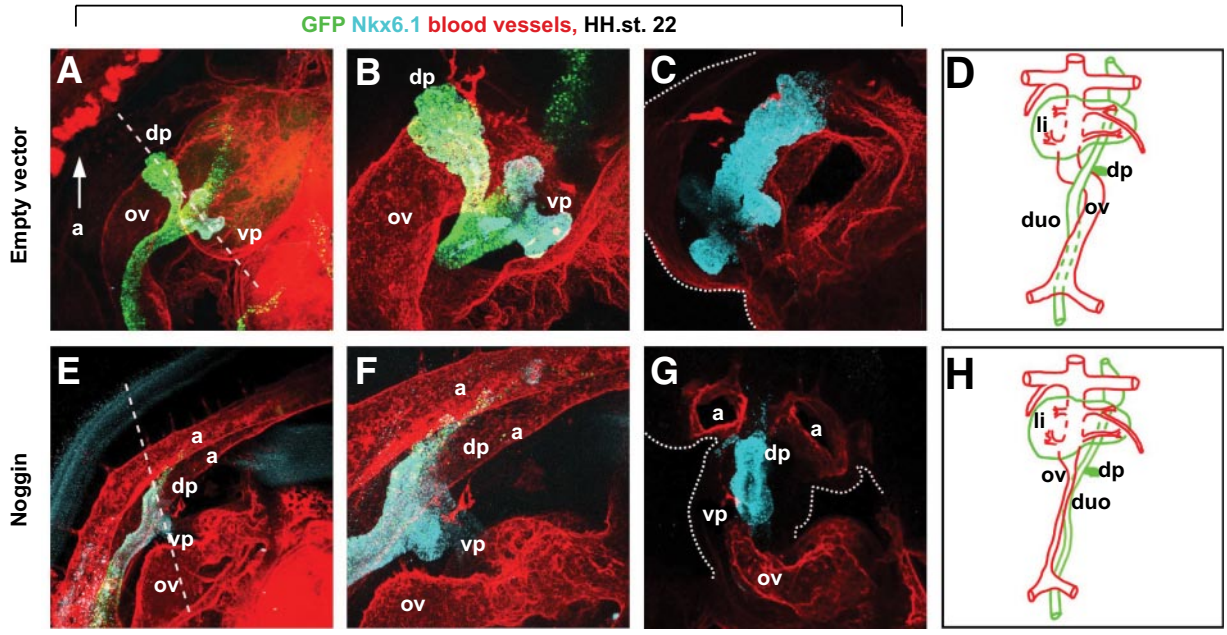

FIG. 8. Vascular/pancreatic development in electroporated embryos 48 h after electroporation. Embryos perfused with a fluorescently-tagged Lens Culinaris Agglutinin (labeling the vascular endothelium) and subjected to whole-mount immunostaing for Nkx6.1 and GFP. *A*,*B* and *E*,*F* show projected z-stacks from lateral views at two different magnifications. *C* and *G*: Projected images from transverse thick vibratome sections from the same embryos (indicated by dashed lines in *A* and *E*). Note how the dorsal aorta is well separated from the pancreas in the control and how the dorsal pancreas curls around the omphalomesenteric vein. In Noggin-electroporated embryos, the omphalomesenteric vein is consistently found ventrally to the pancreas, and in some of the embryos, the paired dorsal aortas fail to fuse. The bisymmetrical mesenchyme is indicated by dashed lines in *F*. (The contrast was temporarily enhanced in the image to allow the drawing based on a background signal. The mesenchyme is not readily observable at the published contrast setting). *D* and *H*: Schematic drawing summarizing the relationship between the gut and pancreas (green) and the omphalomesenteric vein (red). *D* is drawn similar to a study done by Romanoff (33). a, aorta; dp, dorsal pancreas; duo, duodenum; dv, ductus venosus; li, liver; ov, omphalomesenteric vein; vp, ventral pancreas. (A high-quality digital representation of this figure is available in the online issue.)

embryos displayed a duplication of the SPM (supplementary Fig. 5*C* and *D*), suggesting that downregulation of right-sided *Bapx1* expression is required for establishment of the asymmetric SPM.

The observation of precocious endocrine differentiation in Noggin-electroporated embryos prompted us to analyze the expression of *Hes1*. We found that the unbranched tubular dorsal pancreas was *Hes1*-negative 48 h after electroporation, suggesting that the excessive endocrine differentiation is coincident with downregulated *Hes1* expression (Fig. 7*E* and *K*). We therefore looked after 32 h of development and earlier (supplementary Fig. 6 and data not shown). Most of the Nkx6.1-positive dorsal pancreas epithelium had differentiated after 32 h and was *Hes1*-negative, but the remaining Nkx6.1-positive cells expressed normal levels of Hes1. At earlier time points when the pancreas was more normal, we could not detect a general downregulation of *Hes1* in the epithelium (not shown). We can therefore not distinguish between loss of *Hes1* followed by differentiation or vice versa, likely because our ISH protocol does not allow quantitative measurements of mRNA expression levels.

The angiogenic remodeling of major vessels is compromised in Noggin-electroporated embryos. The bilateral expression of *Bapx1* in the mesenchyme of Noggin electroporated embryos was notable. In chicken and mice, the right omphalomesenteric vein is normally found at this position, and the developing pancreas grows around this vessel (4,5). Gene expression changes in this structure might indicate that the normal intimately joined development of the pancreas and the vein was disturbed. To visualize the vasculature and the pancreas, we injected embryos with fluorescently-labeled lens culinaris agglutin, a lectin with high affinity to chicken endothelial cells (20), and subsequently we stained for Nkx6.1 by whole-mount immunohistochemistry (Fig. 8).

At 3 days of development (HH st. 19), the paired omphalomesenteric veins run on each side of the gut tube and join anteriorly at the level of the liver in the ductus venosus (33) (supplementary Fig. 7*C*). The bilateral, ventral Nkx6.1 domains are in close contact to these veins and the dorsal pancreas has grown asymmetrically over the right omphalomesenteric vein (supplementary Fig. 7*C*). At this stage. the dorsal aorta is well separated from the pancreas by the pancreatic mesenchyme. During the next day, a series of anastomoses of the veins occur and most of the left omphalomesenteric vein regresses, leaving behind the right omphalomesenteric vein which curls around the gut at the level of the pancreas (5,33) (supplementary Fig. 7*D* and *F*). The dorsal pancreas and one of the ventral pancreata lie in close contact to the right omphalomesenteric vein (supplementary Fig. 7*F*) (5).

We analyzed the vascular development in control and Noggin electroporated embryos 48 h after electroporation. The electroporated control embryos had normal development of the omphalomesenteric vein (Fig. 8*A*–*C*). Transverse vibratome sectioning revealed the asymmetric pancreas mesenchyme (Fig. 8*C*), and, as expected, the dorsal aorta was well separated from the dorsal pancreas (Fig. 8*A*). In Noggin electroporated embryos, the vasculature developed abnormally (Fig. 8*E*–*G*). The omphalomesenteric vein was found on the ventral side of the pancreas and gut ($n = 6$) and, in some embryos, the dorsal aortas failed to fuse and move dorsally (2 of 6 embryos). To assess the development of the microvasculature, we made *Flk1* ISH on sectioned embryos. This revealed a normal microvasculature around the dorsal pancreas 32 h after electroporation when the omphalomesenteric vein is already displaced to the ventral side in BMP-inhibited embryos (supplementary Fig. 8), suggesting that there is no general inhibition of angiogenesis under these conditions.

DISCUSSION

Development of the pancreas depends on interactions between the epithelium and the mesenchyme as recognized since the studies by Golosow and Grobstein (12), but few endogenous signaling factors have been identified.

Here, we used chicken in ovo endoderm electroporation timed to express the pancreatic transgenes after specification of the pancreas. We reasoned that this would allow us to study BMP signaling during pancreas organogenesis. Detection of pSmad1,5,8 shows that early pancreatic mesenchyme receives a BMP signal, possibly through ALK3, which is expressed in the chicken pancreas mesenchyme (34). Since we find BMP expression in the mesenchyme, it is possible that an autocrine signaling mechanism is occurring. Epithelial expression of the secreted BMP antagonist Noggin resulted in the loss of pSmad1,5,8

immunoreactivity in the adjacent mesenchyme and affected epithelial and mesenchymal development. The epithelium displayed reduced branching, anterior extension of the dorsal pancreas into the stomach mesenchyme, and precocious endocrine differentiation.

Inhibiting BMP signaling compromised angiogenic remodeling that positions the right omphalomesenteric vein adjacent to the pancreas. Instead, we observed a persistence of mesenchymal *Bapx1* expression, a bilateral SMP, and failure of the dorsal aortas to fuse in the most severely affected embryos. We cannot distinguish a direct effect on the endothelial cells from an indirect effect acting through the mesenchyme. However, the microvasculature seems normal in BMP-inhibited embryos, suggesting that some aspects of angiogenesis occur normally and the defect appears limited to major vessels. Notably, the mouse explants corroborate the findings in chick, arguing against involvement of the major vessels. Additionally, mesenchymal Isl1 expression, dependent on signals from blood vessels (35), is maintained.

The results presented herein appear to conflict with a recent report by Goulley et al. (16). In that study, BMP signaling was perturbed by the expression of Noggin and BMP4 in the pancreas epithelium using the *Pdx1* promoter, with no profound effect on pancreatic development. We speculate that this could be due to different levels of expression since establishment of high-expressing transgenic mouse lines used in their studies would be prevented by a severe vascular or pancreatic phenotype caused by embryonic or perinatal lethality, and thus a selection for low expressers. A similar study expressing *Bmp6* under the control of the *Pdx1* promoter resulted in complete pancreas agenesis at a late gestational age, and these mice displayed a hypomorphic spleen, suggesting that the mesenchyme was also affected (15).

The present study suggests that there is no epithelial BMP signaling in the pancreas at the investigated stages, and that the effect on epithelial development is secondary to inhibition of BMP signaling in the mesenchyme. This is supported by the observation that cell autonomous BMP-signaling inhibition in the mouse pancreas mesenchyme leads to an increase in endocrine differentiation concomitant with a decrease in exocrine development. It is possible that the effect of BMP inhibition on the mesenchyme can be subdivided into an inhibition of an autocrine mesenchymal signal and an associated effect on vascular remodelling. BMP signaling in the mesenchyme may be required for the mesenchyme to express a secondary factor acting on the epithelium. Fgf10 is one candidate because mesenchymal Fgf10 is required for epithelial branching and progenitor cell proliferation (9–11). However, there is little Fgf10 expression left at e12.5, the time of explanting in some of the organ culture experiments, suggesting that other factors could be involved.

ACKNOWLEDGMENTS

This work was made possible by grants from the Juvenile Diabetes Research Foundation, the European Union's 6th Framework Program, and the Beta Cell Biology Consortium (grant U19 DK072495).

No potential conflicts of interest relevant to this article were reported.

J.A.-R. designed and carried out all cloning and chicken embryo manipulations and analyses. P.R., C.P.-G., and R.S. generated lentiviral constructs and performed the lentiviral transductions of pancreatic explants and carried out data analysis. J.A.-R. and P.S. conceived the study, participated in its design and coordination, performed data analysis, and drafted the manuscript.

The authors thank Anne Grapin-Botton, Swiss Institute for Experimental Cancer Research, Ecole/Polytechnique Fédérale de Lausanne, and Jacob Hecksher-Sørensen, Hagedorn Research Institute, for helpful discussions, and are grateful to Cliff Tabin, Harvard Medical School, and Richard Harland, University of California, Berkeley, for probes and Noggin cDNA, respectively, and for expert technical help from Malene Jørgensen.

REFERENCES

1. Jorgensen MC, Ahnfelt-Ronne J, Hald J, Madsen OD, Serup P, Hecksher-Sorensen J. An illustrated review of early pancreas development in the mouse. Endocr Rev 2007;28:685–705
2. Hebrok M, Kim SK, Melton DA. Notochord repression of endodermal Sonic hedgehog permits pancreas development. Genes Dev 1998;12:1705–1713
3. Kumar M, Jordan N, Melton D, Grapin-Botton A. Signals from lateral plate mesoderm instruct endoderm toward a pancreatic fate. Dev Biol 2003;259:109–122
4. Lammert E, Cleaver O, Melton D. Induction of pancreatic differentiation by signals from blood vessels. Science 2001;294:564–567
5. Kim SK, Hebrok M, Melton DA. Pancreas development in the chick embryo. Cold Spring Harb Symp Quant Biol 1997;62:377–383
6. Ahnfelt-Ronne J, Hald J, Bodker A, Yassin H, Serup P, Hecksher-Sorensen J. Preservation of proliferating pancreatic progenitor cells by Delta-Notch signaling in the embryonic chicken pancreas. BMC Dev Biol 2007;7:63
7. Apelqvist A, Li H, Sommer L, Beatus P, Anderson DJ, Honjo T, Hrabe de Angelis M, Lendahl U, Edlund H. Notch signalling controls pancreatic cell differentiation. Nature 1999;400:877–881
8. Jensen J, Pedersen EE, Galante P, Hald J, Heller RS, Ishibashi M, Kageyama R, Guillemot F, Serup P, Madsen OD. Control of endodermal endocrine development by Hes-1. Nat Genet 2000;24:36–44
9. Bhushan A, Itoh N, Kato S, Thiery JP, Czernichow P, Bellusci S, Scharfmann R. Fgf10 is essential for maintaining the proliferative capacity of epithelial progenitor cells during early pancreatic organogenesis. Development 2001;128:5109–5117
10. Hart A, Papadopoulou S, Edlund H. Fgf10 maintains notch activation, stimulates proliferation, and blocks differentiation of pancreatic epithelial cells. Dev Dyn 2003;228:185–193
11. Norgaard GA, Jensen JN, Jensen J. FGF10 signaling maintains the pancreatic progenitor cell state revealing a novel role of Notch in organ development. Dev Biol 2003;264:323–338
12. Golosow N, Grobstein C. Epitheliomesenchymal interaction in pancreatic morphogenesis. Dev Biol 1962;4:242–255
13. Wessells NK, Cohen CJ. Early pancreas organogenesis: Morphogenesis, tissue interactions, and mass effects. Dev Biol 1967;15:237–270
14. Hogan BL: Morphogenesis Cell 1999;96:225–233
15. Dichmann DS, Miller CP, Jensen J, Scott Heller R, Serup P. Expression and misexpression of members of the FGF and TGFβ families of growth factors in the developing mouse pancreas. Dev Dyn 2003;226:663–674
16. Goulley J, Dahl U, Baeza N, Mishina Y, Edlund H. BMP4-BMPR1A signaling in β-cells is required for and augments glucose-stimulated insulin secretion. Cell Metab 2007;5:207–219
17. Pedersen JK, Nelson SB, Jorgensen MC, Henseleit KD, Fujitani Y, Wright CV, Sander M, Serup P. Endodermal expression of Nkx6 genes depends differentially on Pdx1. Dev Biol 2005;288:487–501
18. Yokouchi Y, Sakiyama J, Kameda T, Iba H, Suzuki A, Ueno N, Kuroiwa A. BMP-2/-4 mediate programmed cell death in chicken limb buds. Development 1996;122:3725–3734
19. Ahnfelt-Ronne J, Jorgensen MC, Hald J, Madsen OD, Serup P, Hecksher-Sorensen J. An improved method for three-dimensional reconstruction of protein expression patterns in intact mouse and chicken embryos and organs. J Histochem Cytochem 2007;55:925–930
20. Jilani SM, Murphy TJ, Thai SN, Eichmann A, Alva JA, Iruela-Arispe ML. Selective binding of lectins to embryonic chicken vasculature. J Histochem Cytochem 2003;51:597–604
21. Attali M, Stetsyuk V, Basmaciogullari A, Aiello V, Zanta-Boussif MA, Duvillie B, Scharfmann R. Control of beta-cell differentiation by the pancreatic mesenchyme. Diabetes 2007;56:1248–1258

22. Haumaitre C, Lenoir O, Scharfmann R. Histone deacetylase inhibitors modify pancreatic cell fate determination and amplify endocrine progenitors. Mol Cell Biol 2008;28:6373–6383
23. Schmierer B, Hill CS. TGFβ-SMAD signal transduction: molecular specificity and functional flexibility. Nat Rev Mol Cell Biol 2007;8:970–982
24. Faure S, de Santa Barbara P, Roberts DJ, Whitman M. Endogenous patterns of BMP signaling during early chick development. Dev Biol 2002;244:44–65
25. Hamburger VaH, H. L: A series of normal stages in the development of the chick embryo. J Exp. Morphol 1951;88:49–92
26. Matsushita S. Fate mapping study of the endoderm in the posterior part of the 1.5-day-old chick embryo. Dev Growth Differ 1999;41:313–319
27. Grapin-Botton A, Majithia AR, Melton DA. Key events of pancreas formation are triggered in gut endoderm by ectopic expression of pancreatic regulatory genes. Genes Dev 2001;15:444–454
28. Castaing M, Guerci A, Mallet J, Czernichow P, Ravassard P, Scharfmann R. Efficient restricted gene expression in β-cells by lentivirus-mediated gene transfer into pancreatic stem/progenitor cells. Diabetologia 2005;48:709–719
29. Schlueter J, Brand T. Left-right axis development: examples of similar and divergent strategies to generate asymmetric morphogenesis in chick and mouse embryos. Cytogenet Genome Res 2007;117:256–267
30. St Amand TR, Ra J, Zhang Y, Hu Y, Baber SI, Qiu M, Chen Y. Cloning and expression pattern of chicken Pitx2: a new component in the SHH signaling pathway controlling embryonic heart looping. Biochem Biophys Res Commun 1998;247:100–105
31. Hecksher-Sorensen J, Watson RP, Lettice LA, Serup P, Eley L, De Angelis C, Ahlgren U, Hill RE. The splanchnic mesodermal plate directs spleen and pancreatic laterality, and is regulated by Bapx1/Nkx3.2. Development 2004;131:4665–4675
32. Asayesh A, Sharpe J, Watson RP, Hecksher-Sorensen J, Hastie ND, Hill RE, Ahlgren U. Spleen versus pancreas: strict control of organ interrelationship revealed by analyses of Bapx1-/- mice. Genes Dev 2006;20:2208–2213
33. Romanoff AL: *The Avian Embryo*, *Structural and Functional Development*. New York: Macmillan Company, 1960
34. Smith DM, Nielsen C, Tabin CJ, Roberts DJ. Roles of BMP signaling and Nkx2.5 in patterning at the chick midgut-foregut boundary. Development 2000;127:3671–3681
35. Jacquemin P, Yoshitomi H, Kashima Y, Rousseau GG, Lemaigre FP, Zaret KS. An endothelial-mesenchymal relay pathway regulates early phases of pancreas development. Dev Biol 2006;290:189–199